

# We are IntechOpen, the world's leading publisher of Open Access books Built by scientists, for scientists

6,900

Open access books available

186,000

International authors and editors

200M

Downloads

Our authors are among the

154

Countries delivered to

TOP 1%

most cited scientists

12.2%

Contributors from top 500 universities



WEB OF SCIENCE™

Selection of our books indexed in the Book Citation Index  
in Web of Science™ Core Collection (BKCI)

Interested in publishing with us?  
Contact [book.department@intechopen.com](mailto:book.department@intechopen.com)

Numbers displayed above are based on latest data collected.  
For more information visit [www.intechopen.com](http://www.intechopen.com)



---

# Investigation of Hydraulic and Natural Fracture Interaction: Numerical Modeling or Artificial Intelligence?

---

Reza Keshavarzi and Reza Jahanbakhshi

Additional information is available at the end of the chapter

<http://dx.doi.org/10.5772/56382>

---

## Abstract

Hydraulic fracturing of naturally fractured reservoirs is a critical issue for petroleum industry, as fractures can have complex growth patterns when propagating in systems of natural fractures. Hydraulic and natural fracture interaction may lead to significant diversion of hydraulic fracture paths due to intersection with natural fractures which causes difficulties in proppant transport and eventually job failure. In this study, a comparison has been made between numerical modeling and artificial intelligence to investigate hydraulic and natural fracture interaction. First of all an eXtended Finite Element Method (XFEM) model has been developed to account for hydraulic fracture propagation and interaction with natural fracture in naturally fractured reservoirs including fractures intersection criteria into the model. It is assumed that fractures are propagating in an elastic medium under plane strain and quasi-static conditions. Comparison of the numerical and experimental studies results has shown good agreement. Secondly, a feed-forward with back-propagation artificial neural network approach has been developed to predict hydraulic fracture path (crossing/turning into natural fracture) due to interaction with natural fracture based on experimental studies. Effective parameters in hydraulic and natural fracture interaction such as in situ horizontal differential stress, angle of approach, interfacial coefficient of friction, young's modulus of the rock and flow rate of fracturing fluid are the inputs and hydraulic fracturing path (crossing/turning into natural fracture) is the output of the developed artificial neural network. The results have shown high potentiality of the developed artificial neural network approach to predict hydraulic fracturing path due to interaction with natural fracture. Finally, both of the approaches have been examined by a set of experimental study data and the results have been compared. It is clearly observed that both of them yield promising results

while numerical modeling yields more detailed results which can be used for further investigations but it is computationally more expensive and time-consuming than artificial neural network approach. On the other hand, since artificial neural network approach is mainly data-driven if just the input data is available (even while fracturing) the hydraulic fracture path (crossing/turning into natural fracture) can be predicted real-time and at the same time that fracturing is happening.

## 1. Introduction

Hydraulic fracture growth through naturally fractured reservoirs presents theoretical, design, and application challenges since hydraulic and natural fracture interaction can significantly affect hydraulic fracturing propagation. Although hydraulic fracturing has been used for decades for the stimulation of oil and gas reservoirs, a thorough understanding of the interaction between induced hydraulic fractures and natural fractures is still lacking. This is a key challenge especially in unconventional reservoirs, because without natural fractures, it is not possible to recover hydrocarbons from these reservoirs. Meanwhile, natural fracture systems are important and should be considered for optimal stimulation. For naturally fractured formations under reservoir conditions, natural fractures are narrow apertures which are around  $10^{-5}$  to  $10^{-3}$  m wide and have high length/width ratios ( $>1000:1$ ) [1]. Typically natural fractures are partially or completely sealed but this does not mean that they can be ignored while designing well completion processes since they act as planes of weakness reactivated during hydraulic fracturing treatments that improves the efficiency of stimulation [2]. The problem of hydraulic and natural fracture interaction has been widely investigated both experimentally [3, 4, 5, 6, 7, 8] and numerically [9, 10, 11, 12, 13, 14, 15, 16, 17, 18]. Many field experiments also demonstrated that a propagating hydraulic fracture encountering natural fractures may lead to arrest of fracture propagation, fluid flow into natural fracture, creation of multiple fractures and fracture offsets [19, 20, 21, 22] which will result in a reduced fracture width. This reduction in hydraulic fracture width may cause proppant bridging and consequent premature blocking of proppant transport (so-called screenout) [23, 24] and finally treatment failure. Although various authors have provided fracture interaction criteria [4, 5, 25] determining the induced fracture growth path due to interaction with pre-existing fracture and getting a viewpoint about variable or variables which have a decisive impact on hydraulic fracturing propagation in naturally fractured reservoirs is still unclear and highly controversial. However, experimental studies have suggested that horizontal differential stress, angle of approach and treatment pressure are the parameters affecting hydraulic and natural fracture interaction [4, 5, 6] but a comprehensive analysis of how different parameters influence the fracture behavior has not been fully investigated to date. In this way, in order to assess the outcome of hydraulic fracture stimulation in naturally fractured reservoirs the following questions should be answered:

What is the direction of hydraulic fracture propagation?

How will the propagating hydraulic fracture interact with the natural fracture?

Will the advancing hydraulic fracture cross the natural fracture or will it turn into it?

For the purpose of this study, a 2D eXtended finite element method (XFEM) has been compared with a feed-forward with back-propagation artificial neural network approach to account for hydraulic and natural fracture interaction.

## 2. Interaction between hydraulic and natural fractures

The interaction between pre-existing natural fractures and the advancing hydraulic fracture is a key issue leading to complex fracture patterns. Large populations of natural fractures are sealed by precipitated cements (Figure 1) which are weakly bonded with mineralization that even if there is no porosity in the sealed fractures, they may still serve as weak paths for the growing hydraulic fractures [2].

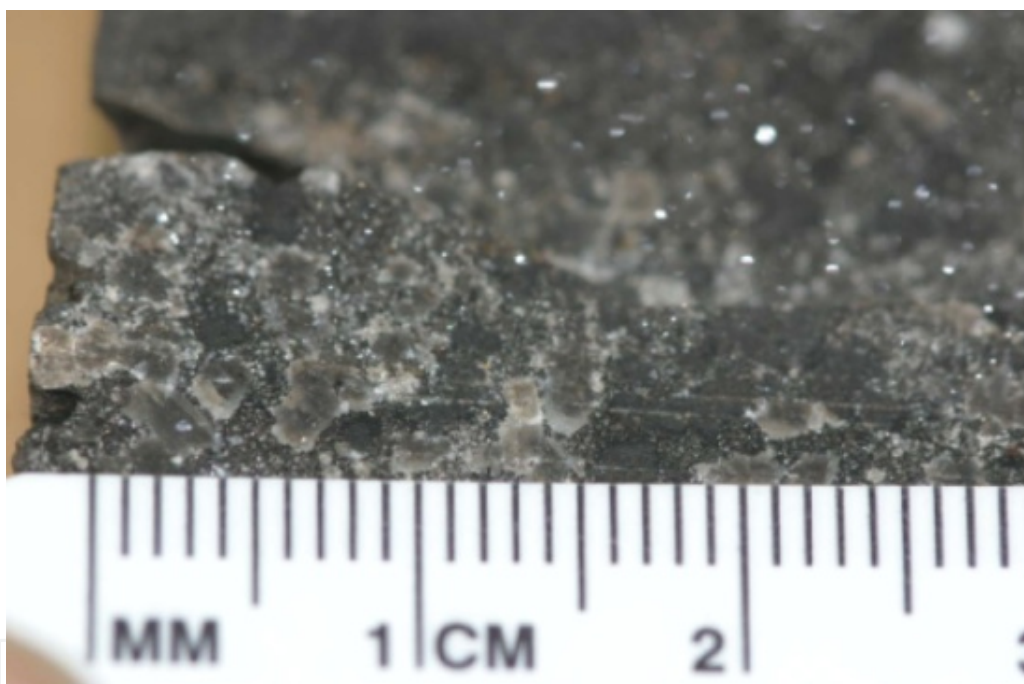


**Figure 1.** A weakly bonded fracture cement in a shale sample [26].

In this way, experimental studies [4, 5, 6] suggested several possibilities that may occur during hydraulic and natural fractures interaction. Blanton [4] conducted some experiments on naturally fractured Devonian shale as well as blocks of hydrostone in which the angle of approach and horizontal differential stress were varied to analyze hydraulic and natural fracture interaction in various angles of approach and horizontal differential stresses. He concluded that any change in angle of approach and horizontal differential stress can affect hydraulic fracture propagation behavior when it encounters a natural fracture which will be referred to as opening, arresting and crossing. Warpinski and Teufel [5] investigated the effect of geologic discontinuities on hydraulic fracture propagation by conducting mineback

experiments and laboratory studies on Coconino sandstone having pre-existing joints. They observed three modes of induced fracture propagation which were crossing, arrest by opening the joint and arrest by shear slippage of the joint with no dilation and fluid flow along the joint. In 2008 [6] some laboratory experiments were performed to investigate the interaction between hydraulic and natural fractures. They also observed three types of interactions between hydraulic and pre-existing fractures which were the same as Warpinski and Teufel's observations. The above referenced experimental studies have investigated the initial interaction between the induced fracture and the natural fracture, however, in reality may be the hydraulic fracture is arrested by natural fracture temporarily but with continued pumping of the fluid, the hydraulic fracture may cross (Figure 2) or turn into the natural fracture (Figure 3).

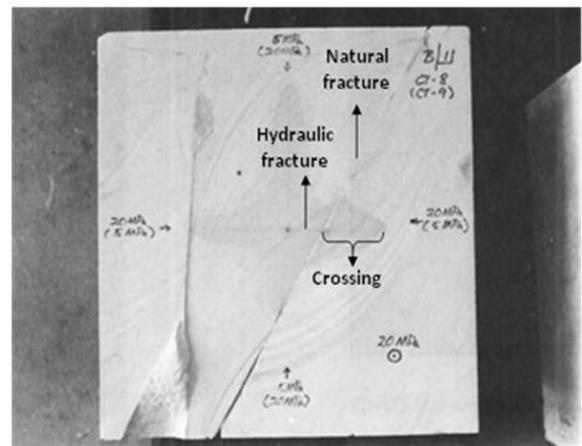
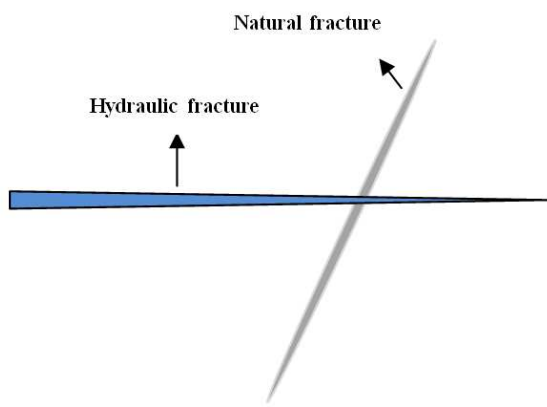


**Figure 2.** Propagating hydraulic fracture crosses the natural fracture and keep moving without any significant change in its path: left image is a schematic view of crossing and right image is the result of experimental study [4].

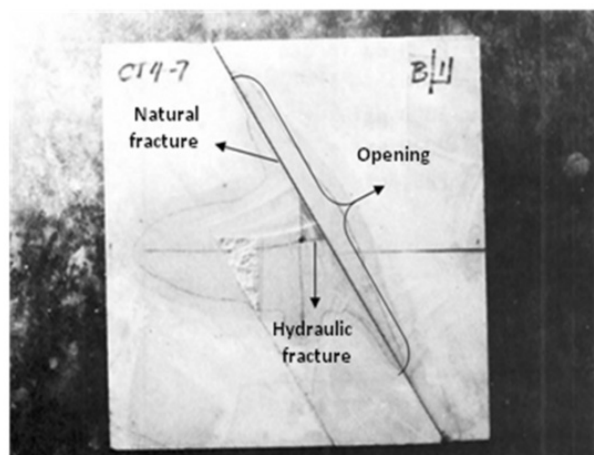
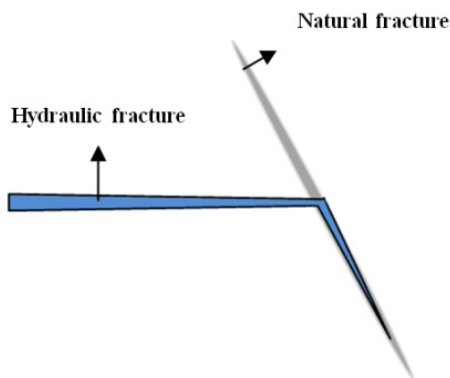


**Figure 3.** Hydraulic fracture turns into the natural fracture and propagates along it: left image is a schematic view and right image is the result of experimental study [4].

Alternatively, in some cases the hydraulic fracture may get arrested if the natural fracture is long enough and favorably oriented to accept and divert the fluid.

### 3. Numerical modeling: Extended Finite Element Method (XFEM)

For fracture propagation through numerical modeling an energy based criterion has been considered which is energy release rate,  $G$ . The energy release rate,  $G$ , is related to the stress intensity factors through Eq. 1 [27]:

$$G = \frac{1}{E'}(K_I^2 + K_{II}^2) \quad (1)$$

where  $E' = E$  for plane stress ( $E$  is Young's modulus) and  $E' = E/(1- \nu^2)$  for plane strain (where  $\nu$  is the Poisson's ratio). Energy release rate has been calculated by the  $J$  integral using the domain integral approach [28] whereas  $J$  integral is equivalent to the definition of the fracture energy release rate,  $G$ , for linear elastic medium. If the  $G$  is greater than a critical value,  $G_c$ , the fracture will propagate critically. The direction of hydraulic fracture propagation will be calculated by Eq. 2 [29]:

$$\theta_c = 2 \tan^{-1} \frac{1}{4} \left( \frac{K_I}{K_{II}} \pm \sqrt{\left( \frac{K_I}{K_{II}} \right)^2 + 8} \right) \quad (2)$$

During hydraulic and natural fracture interaction at the intersection point the hydraulic fracture has more than one path to follow which are crossing and turning into natural fracture. The most likely path is the one that has the maximum  $G$ . So, at the intersection point energy release rate is calculated for both crossing ( $G_{cross}$ ) and turning into natural fracture ( $G_{turn}$ ), and if  $(G_{turn}/G_{cross}) > 1$  hydraulic fracture turns into natural fracture while if  $(G_{turn}/G_{cross}) < 1$  crossing takes place and hydraulic fracture crosses the natural fracture. To examine the proposed mechanism, eXtended Finite Element method (XFEM) was applied which was first introduced by Belytschko and Black [30] in order to avoid explicit modeling of discrete cracks by enhancing the basic finite element solution. In comparison to the classical finite element method, XFEM provides significant benefits in the numerical modeling of fracture propagation and it overcomes the difficulties of the conventional finite element method for fracture analysis, such as restriction in remeshing after fracture growth and being able to consider arbitrary varying geometry of fractures [12]. XFEM enhances the basic finite element solution through the use of enrichment functions which are the Heaviside function for elements that are completely cut by the crack and Westergaard-type asymptotic functions for elements containing crack-tips [27]. The displacement field for a point "x" inside the domain can be approximated based on the XFEM formulation as below [31]:

$$u^h(x) = \sum_{I \in N_{nu}} N_I(x) \left( u_I + \underbrace{H(x)a_I}_{I \in N_{ua}} + \underbrace{\sum_{\alpha=1}^4 F_\alpha(x)b_I^\alpha}_{I \in N_{ub}} \right) \quad (3)$$

Where  $N_I$  is the finite element shape function,  $u_I$  is the nodal displacement vector associated with the continuous part of the finite element solution,  $H(x)$  is the Heaviside enrichment function where it takes the value +1 above the crack and -1 below the crack,  $a_I$  is the nodal enriched degree of freedom vector associated with the Heaviside (discontinuous) function,  $F_\alpha(x)$  is the near-tip enrichment function,  $b_I^\alpha$  is the nodal enriched degree of freedom vector associated with the asymptotic crack-tip function,  $N_u$  is the set of all nodes in the domain,  $N_\alpha$  is the subset of nodes enriched with the Heaviside function and  $N_b$  is the subset of nodes enriched with the near tip functions. At the intersection point, instead of Heaviside enrichment function, Junction function will be applied as shown in Figure 4 [32]. By all means, XFEM is well-suited for modeling hydraulic fracture propagation and diversion in the presence of natural fracture.

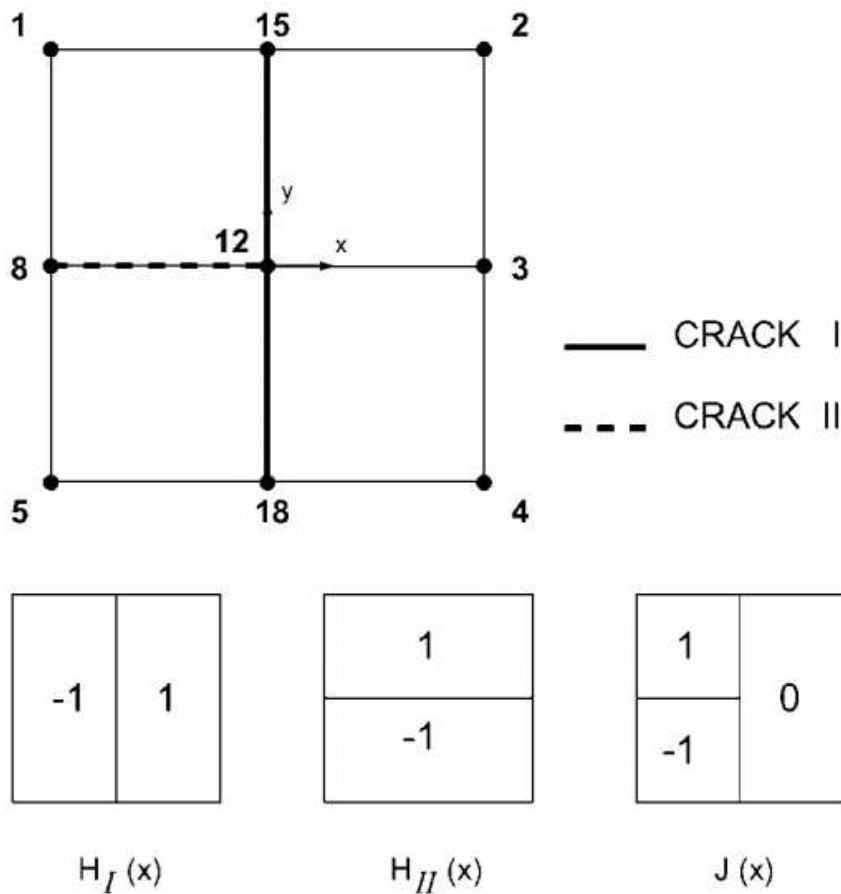
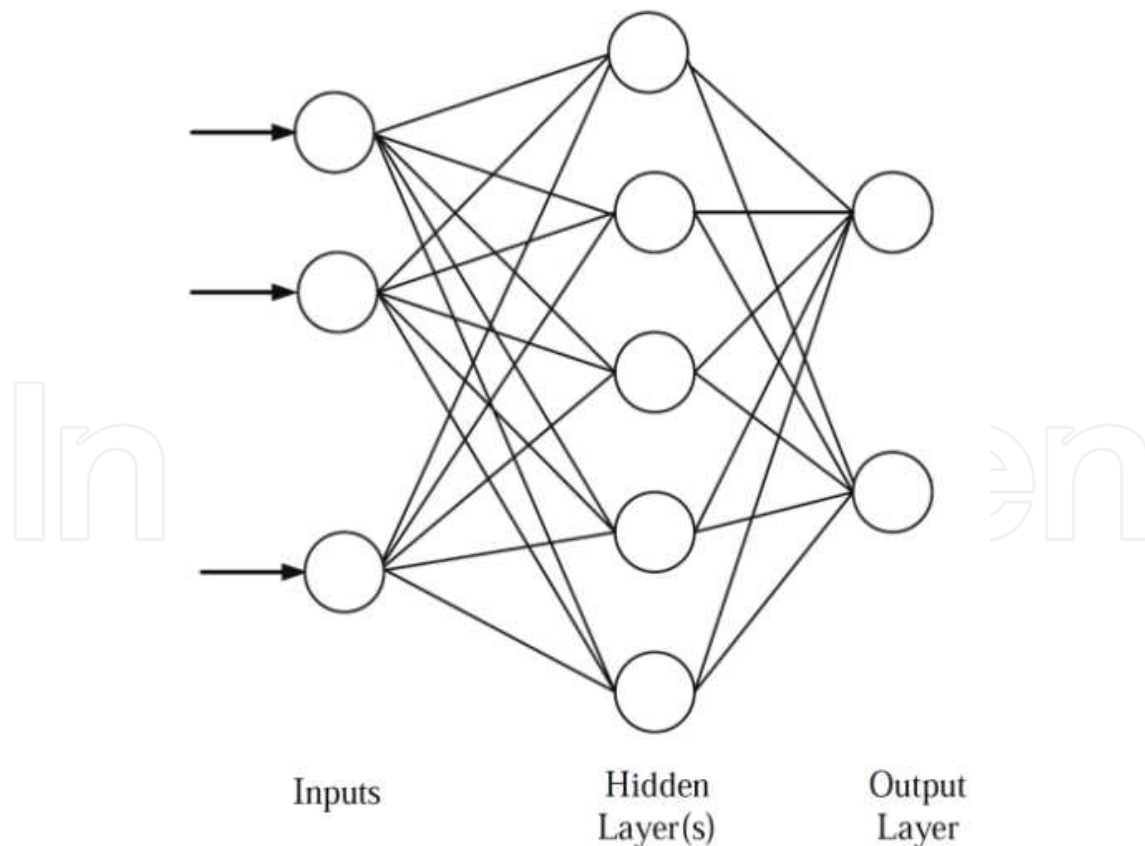


Figure 4. Definition of Junction function at the intersection point [32].

#### 4. Artificial intelligence: Artificial Neural Network (ANN)

Artificial Neural Network (ANN) is considered as a different paradigm for computing and is being successfully applied across an extraordinary range of problem domains, in all areas of engineering. ANN is a non-linear mapping structure based on the function of the human brain that can solve complicated problems related to non-linear relations in various applications which makes it superior to conventional regression techniques [33, 34]. ANNs are capable of distinguishing complex patterns quickly with high accuracy without any assumptions about the nature and distribution of the data and they are not biased in their analysis. The most important aspect of ANNs is their capacity to realize the patterns in obscure and unknown data that are not perceptible to standard statistical methods. Statistical methods use ordinary models that need to add some terms to become flexible enough to satisfy experimental data, but ANNs are self-adaptable. The structure of the neural network is defined by the interconnection architecture between the neurons which are grouped into layers. A typical ANN mainly consists of an input layer, an output layer, and hidden layer(s) (Figure 5). As shown in Figure 5, each neuron of a layer is connected to each neuron of the next layer. Signals are passed between neurons over the connecting links. Each connecting link has an associated weight which multiplies by the related input.



**Figure 5.** Schematic structure of an ANN.

Also, to diversify the various processing elements, a bias is added to the sum of weighted inputs called net input shown in Eq. (4)

$$n = (w_{s,1}p_1 + w_{s,2}p_2 + w_{s,3}p_3 + \dots + w_{s,R}p_R) + b_s \tag{4}$$

Where  $n$  is the net input,  $w$  is the weight,  $p$  is the input,  $b$  is the bias,  $S$  is the number of neurons in the current layer and  $R$  is the number of neurons in the previous layer.

Each neuron applies an activation function to its input to determine its output signal [35]. Neurons may use any differentiable activation function to generate their output based on problem requirement. The most useful activation functions are as follows:

$$a = \text{purelin}(n) = n \tag{5}$$

$$a = \text{tansig}(n) = \left( \frac{2}{1 + \exp(-2n)} \right) - 1 \tag{6}$$

$$a = \text{radbas}(n) = \exp(-n^2) \tag{7}$$

where  $a$  is the neuron layer output. Purelin is a linear activation function (Figure 6A) defined in Eq. (5). Tansig is hyperbolic tangent sigmoid activation function (Figure 6B) mathematically shown in Eq. (6). Radbas is Gaussian activation function (Figure 6C) shown in Eq. (7). In Figure. 7, a one layer network with  $R$  inputs and  $S$  neurons is shown [36]. The optimum number of hidden layers and the number of neurons in these layers are determined by trial and error during the training/learning process. The hidden layers in the network are used to develop the relationship between the variables. In general, multilayer networks are more powerful than single-layer networks [37].

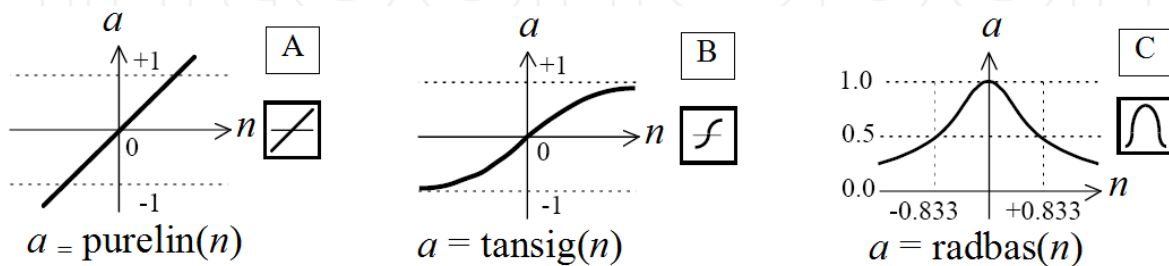
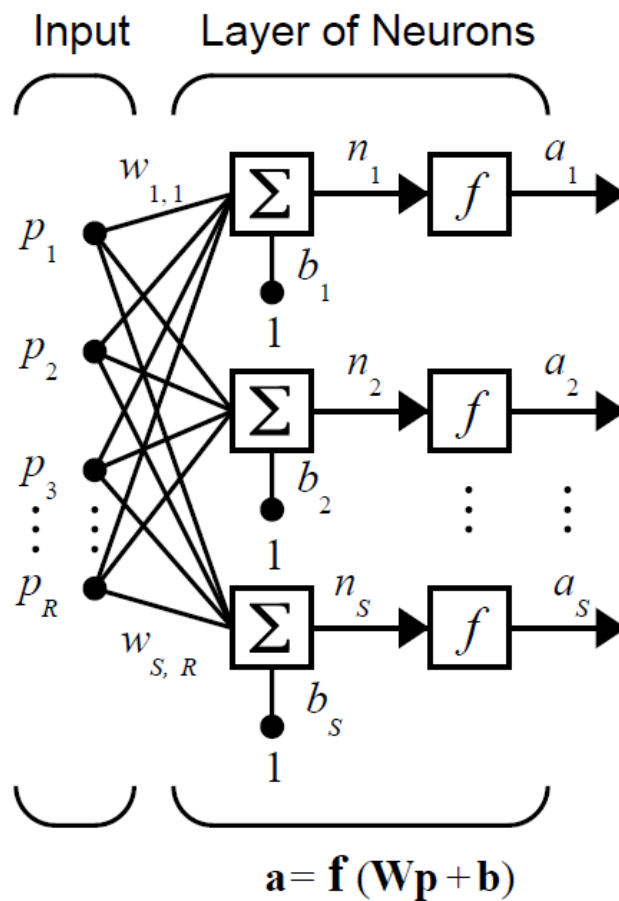


Figure 6. Common Activation functions.



**Figure 7.** A one layer network architecture with “R” inputs and “S” neurons.

#### 4.1. Feed-forward network with back-propagation

The feed-forward network with back-propagation (FFBP) is one of the most eminent and widespread ANNs in engineering applications [38]. In addition, it is easy to implement and solves many types of problems correctly [39]. Usually, FFBP uses tansig and purelin as activation functions in the hidden and output layers, respectively and the net input is calculated the same as Eq. 4. FFBP operates in two steps. First, the phase in which the input information at the input nodes is propagated forward to compute the output information signal at the output layer. In other words, in this step the input data are presented to the input layer and the activation functions process the information through the layers until the network’s response is generated at the output layer. Second, the phase in which adjustments to the connection strengths are made based on the differences between the computed and observed information signals at the output. In this step, the network’s response is compared to the desired output and if it does not agree, an error is generated. The error signals are then transmitted back from the output layer to each node in the hidden layer(s) [40]. Then, based on the error signals received, connection weights between layer neurons and biases are updated. In this way, the network learns to reproduce outputs by learning patterns contained within the data. One iteration of this algorithm can be written as Eq. 8:

$$X_{k+1} = X_k - \alpha_k g_k \quad (8)$$

where  $X_k$  is a vector of current weights and biases,  $g_k$  is the current gradient, and  $\alpha_k$  is the learning rate. Once the network is trained, it can then make predictions from a new set of inputs that was not used to train the network.

#### 4.2. ANN performance criteria

There are several quantitative measures to assess ANN performance that the most usual one in a binary classification test is accuracy [41] (Fawcett 2006). To understand the meaning of accuracy, some definitions like true positive, false positive, true negative and false negative should be explained. Imagine a scenario where the occurrence of an event is considered. The test outcome can be positive (occurrence of the event) or negative (the event doesn't occur). According to this scenario:

- True Positive (TP): The event occurs and it is correctly diagnosed as it occurs;
- False Positive (FP): The event doesn't occur but it is incorrectly diagnosed as it occurs;
- True Negative (TN): The event doesn't occur and it is correctly diagnosed as it doesn't occur;
- False Negative (FN): The event occurs but it is incorrectly diagnosed as it doesn't occur.

According to above definitions:

$$\text{Accuracy} = (\text{TP} + \text{TN}) / (\text{TP} + \text{TN} + \text{FP} + \text{FN}) \quad (9)$$

In general, the accuracy of a system is a degree of closeness of the measured values to the actual (true) values [42].

## 5. Results and discussions

Physically, modeling hydraulic fracturing is a complicated phenomenon due to the heterogeneity of the earth structure, in-situ stresses, rock behavior and the physical complexities of the problem, hence if natural fractures are added up to the problem it gets much more complex in both field operation and numerical aspects. For simplicity, it is assumed that rock is a homogeneous isotropic material and the fractures are propagating in an elastic medium under plane strain and quasi-static conditions driven by a constant and uniform net pressure throughout the hydraulic fracture system. Fracturing fluid pressure is included in the model by putting force tractions on the necessary degrees of freedom along the fracture. A schematic illustration for the problem has been presented in Figure 8 which shows that hydraulic fracture propagates toward the natural fracture and intersects with it at a specific angle of approach,  $\theta$ , and in-situ horizontal differential stress,  $(\sigma_1 - \sigma_3)$ .

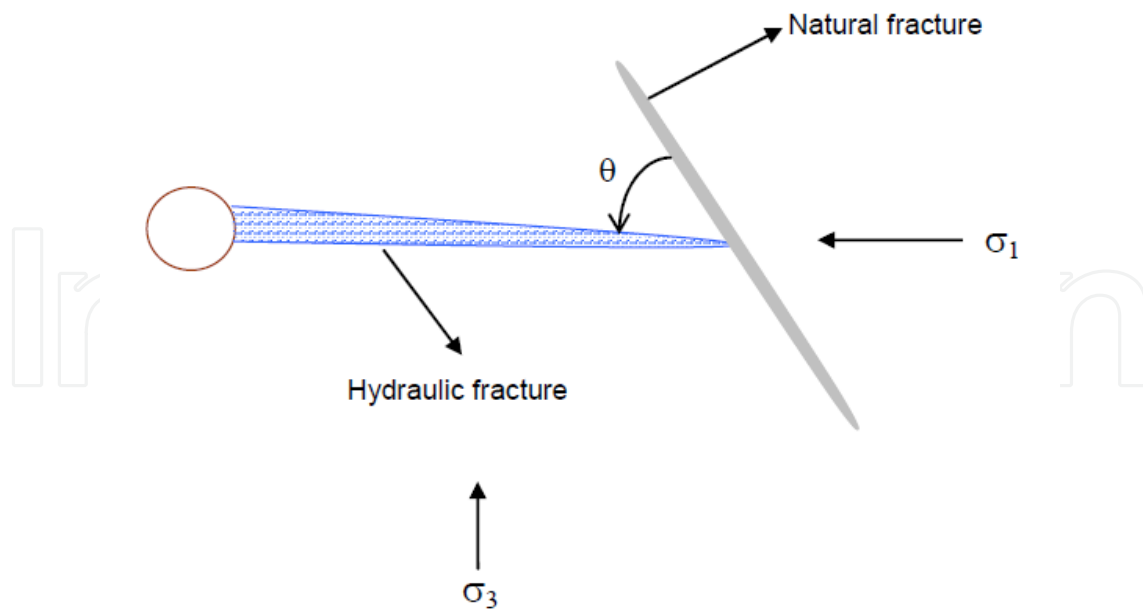


**Figure 8.** Schematic of hydraulic fracture intersecting pre-existing natural fracture [24].

So, a 2D XFEM code has been developed to model hydraulic fracture propagation in naturally fractured reservoirs and interaction with natural fractures. For this purpose, firstly Warpinski and Teufel’s [5] experiments have been modeled to see how much the results of the developed XFEM model for hydraulic and natural fracture interaction, are compatible with them. Table 1, presents the results of XFEM code which can be compared with Warpinski and Teufel’s [5] experiments. As shown in Table 1, the results of XFEM code indicate that at high to medium angles of approach, crossing and turning into natural fracture both are observed depending on the differential stress while at low angles of approach with low to high differential stress, the predominant case during hydraulic and natural fracture interaction is hydraulic fracture diversion along natural fracture which are in good agreement with Warpinski and Teufel’s [5] experiments.

Angle of approach ( $\theta^\circ$ )	Max. horizontal stress (psi)	min. horizontal stress (psi)	Horizontal differential stress (psi)	Experimental results [5]	$G_{turn}/G_{cross}$	XFEM results
30	1000	500	500	Turn into	3.46	Turn into
30	1500	500	1000	Turn into	2.05	Turn into
30	2000	500	1500	Turn into	1.29	Turn into
60	1000	500	500	Turn into	1.948	Turn into
60	1500	500	1000	Turn into	1.201	Turn into
60	2000	500	1500	Crossing	0.785	Crossing
90	1000	500	500	Turn into	1.013	Turn into
90	1500	500	1000	Crossing	0.833	Crossing
90	2000	500	1500	Crossing	0.598	Crossing

**Table 1.** Comparison of XFEM code results with Warpinski and Teufel’s [5] experiments

Meanwhile debonding of natural fracture prior to hydraulic and natural fracture intersection could also be modeled which is a complicated and very interesting phenomena that has been rarely investigated. Figure 9, presents pre-existing fracture debonding before intersection with hydraulic fracture at approaching angles of  $30^\circ$ ,  $60^\circ$ ,  $90^\circ$  in Warpinski and Teufel's [5] experiments. As it is clearly observed in stress maps in Figure 9, a tensile stress is exerted ahead of hydraulic fracture tip for all of the approaching angles which makes the natural fracture debonded. In addition, the length and the position of the debonded zone vary depending on natural fracture orientation and horizontal differential stress.

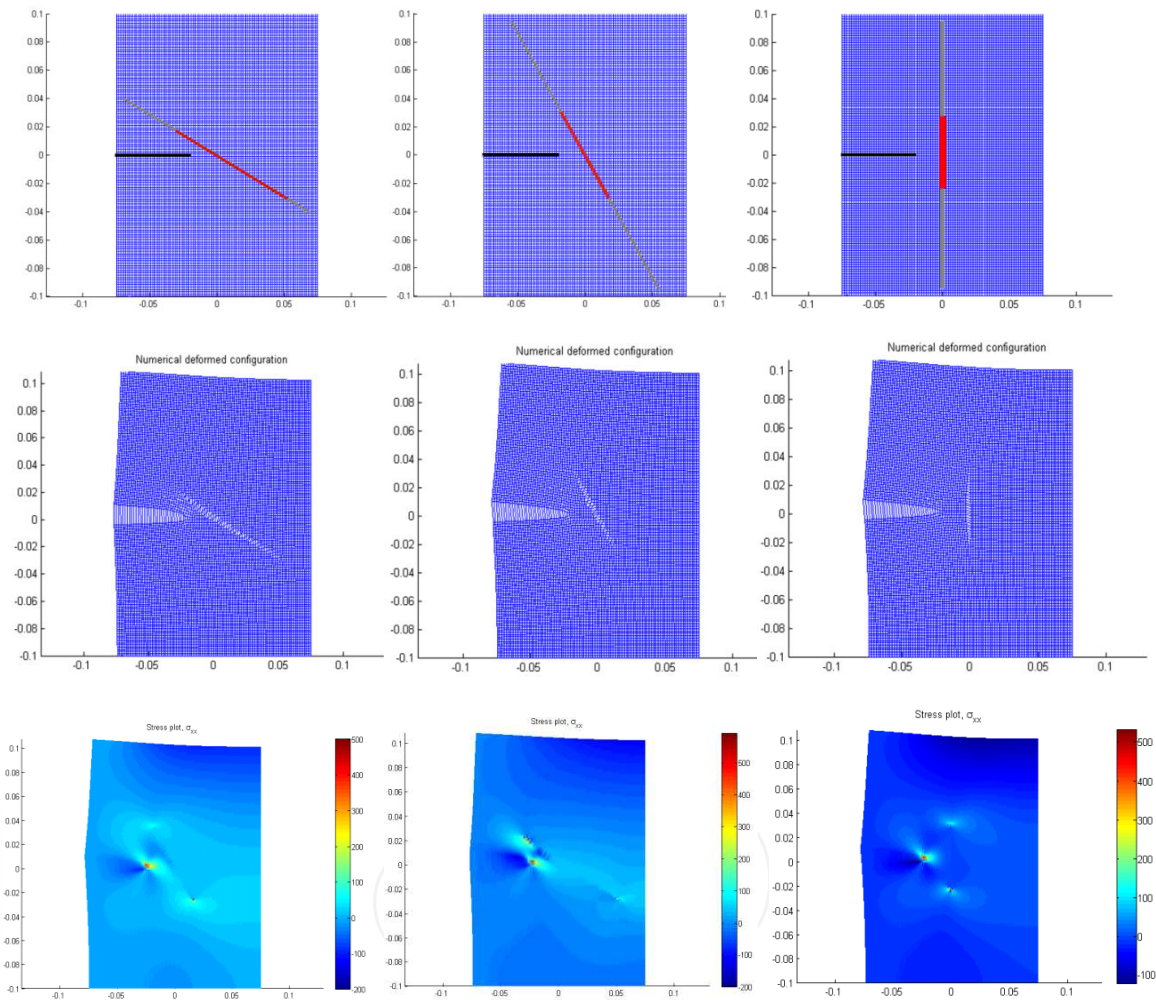


**Figure 9.** Natural fracture debonding before intersecting with hydraulic fracture at  $30^\circ$  (horizontal differential stress=1500 psi),  $60^\circ$  (horizontal differential stress=1000 psi),  $90^\circ$  (horizontal differential stress=1500 psi): the upper images show the coordinates of hydraulic and natural fracture relative to each other where the debonded zones are highlighted in red, the middle images they are the numerical deformed configurations (magnified by 3) and the images below them are the stress maps ( $\sigma_{xx}$ ) (magnified by 3).

Figure 10, shows the debonded zone at the intersecting point of hydraulic and natural fracture and Figure 11 presents the result of hydraulic and natural fracture interaction for approaching angles of  $30^\circ$ ,  $60^\circ$ ,  $90^\circ$ .

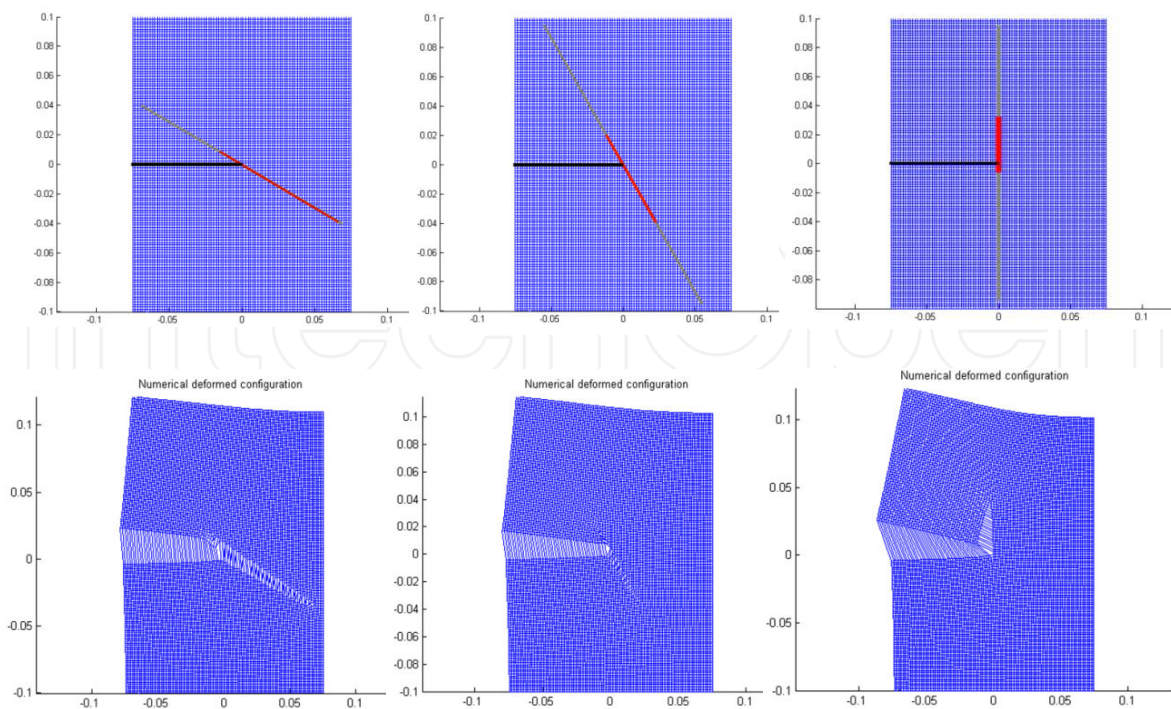


**Figure 10.** Debonded zones (highlighted in red) of natural fracture at the intersecting point with hydraulic fracture at 30° (horizontal differential stress=1500 psi), 60° (horizontal differential stress=1000 psi), 90° (horizontal differential stress=1500 psi): the upper images show the coordinates of hydraulic and natural fracture relative to each other where the debonded zones are highlighted in red and the images below them are the numerical deformed configurations (magnified by 3).

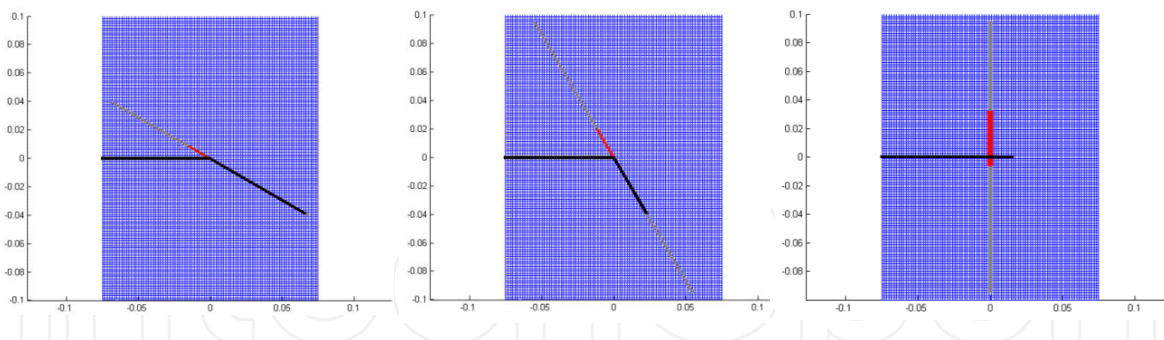


**Figure 11.** The results of hydraulic and natural fracture interaction after intersection: the left image is a natural fracture with the orientation of 30° (horizontal differential stress=1500 psi), the middle image is a natural fracture with the orientation of 60° (horizontal differential stress=1000 psi) and the right image shows a natural fracture with the orientation of 90° (horizontal differential stress=1500 psi).

In the second step, a FFBP neural network has been applied for predicting growing hydraulic fracturing path due to interaction with natural fracture in such a way that horizontal differential stress, angle of approach, interfacial coefficient of friction, young's modulus of the rock and flow rate of fracturing fluid are the inputs and hydraulic fracturing path (crossing or turning into natural fracture) is the output whereas tansig is an activation function. The data

set used in this model consists of around 100 data based on experimental studies [4, 5, 6]. Table 2, represents the range of the parameters used in the developed ANN.

Parameter	Min	Max
Horizontal differential stress (psi)	290	2175
Angle of approach (deg)	30	90
Interfacial coefficient of friction	0.38	1.21
Young's modulus of the rock (psi)	$1.218 \times 10^6$	$1.45 \times 10^6$
Flow rate of fracturing fluid ( $\text{m}^3/\text{s}$ )	$4.2 \times 10^{-9}$	$8.2 \times 10^{-7}$

**Table 2.** Range of the parameters used in the FFBP model.

The data in the database were randomly divided into two subsets. The training subset used 70% and the remaining 30%, was used for the testing subset. For standardizing the range of the input data and improves the training process the data used in network development were pre-processed by normalizing. Normalizing the data enhances the fairness of training by preventing an input with large values from swamping out another input that is equally important but with smaller values [43]. The optimal number of the neurons of a single hidden layer network for the developed ANN using trial and error method based on accuracy is 19 which is shown in Table 3. The developed FFBP neural network represented a high accuracy of 96.66% which was so promising. Also, according to the dataset, around 30 data were assigned for testing subset. Figure 12, show the results of the developed FFBP neural network predictions with actual measurements for testing subset.

Number of hidden neurons	Accuracy (%)
10	83.33
11	90
12	86.67
13	80
14	90
15	83.33
16	83.33
17	90
18	93.33
19	96.66
20	90

**Table 3.** Developed FFBP model designing with different neurons in the hidden layer.

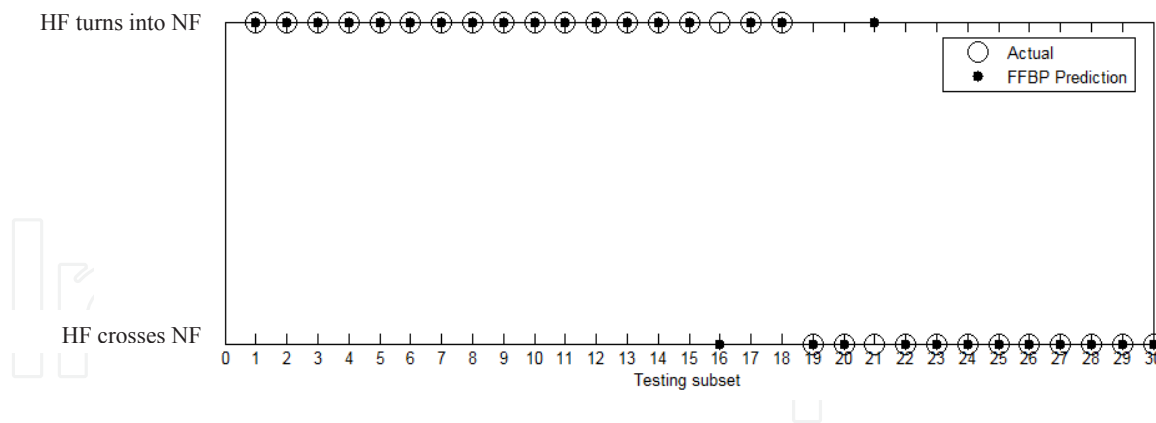


**Figure 12.** Comparison between actual case and FFBP prediction for testing subset.

As shown in Figure 12, FFBP predictions are in prominent agreement with actual measurements which shows the high efficiency of the developed FFBP neural network approach for predicting hydraulic fracturing path due to interaction with natural fracture based on horizontal differential stress, angle of approach, interfacial coefficient of friction, young’s modulus of the rock and flow rate of fracturing fluid. Finally, both XFEM and ANN approaches have been examined by a set of experimental study data [4, 6] and the results have been compared. The results of a comparison are presented in Table 4. As shown in Table 4 both of the proposed approaches yield quite promising results and in just one case ANN approach result doesn’t agree with the actual case.

Horizontal Differential Stress (psi)	Angle of approach (deg)	Coefficient of friction	E*10 <sup>6</sup> (psi)	Flow rate of fracturing fluid (m <sup>3</sup> /s)	Actual Case	XFEM Result	FFBP Prediction
290	60	0.6	1.45	8.2 e-7	T*	T	T
1885	45	0.6	1.45	8.2 e-7	T	T	T
1340	30	0.68	1.3	1 e-7	T	T	T
410	90	0.68	1.3	1 e-7	T	T	T
725	60	0.38	1.218	4 e-9	T	T	T
1015	30	0.38	1.218	4 e-9	T	T	T
913.5	60	0.38	1.218	4 e-9	T	T	C*
2175	60	0.6	1.45	8.2 e-7	C	C	C
1522.5	90	0.89	1.218	4 e-9	C	C	C
1595	90	0.89	1.218	4 e-9	C	C	C

\* T= Turning into natural fracture

\* C= Crossing natural fracture

**Table 4.** Comparison between actual case, XFEM results and FFBP prediction

## 6. Conclusions

Two new numerical modeling and artificial intelligence methodologies were introduced and compared to account for hydraulic and natural fracture interaction. First a new approach has been proposed through XFEM model and an energy criterion has been applied to predict hydraulic fracture path due to interaction with natural fracture. To validate and show the efficiency of the developed XFEM code, firstly the results obtained from XFEM model have been compared with experimental studies which shows good agreement. It's been concluded that natural fracture most probably will divert hydraulic fracture at low angles of approach while at high horizontal differential stress and angles of approach of 60 or greater, the hydraulic fracture crosses the natural fracture. Meanwhile, the growing hydraulic fracture exerts large tensile stress ahead of its tip which leads to debonding of sealed natural fracture before intersecting with hydraulic fracture that is a key point to demonstrate hydraulic and natural fracture behaviors before and after intersection. Then, a FFBP neural network was developed based on horizontal differential stress, angle of approach, interfacial coefficient of friction, young's modulus of the rock and flow rate of fracturing fluid and the ability and efficiency of the developed ANN approach to predict hydraulic fracturing path due to interaction with natural fracture was represented. The results indicate that the developed ANN is not only feasible but also yields quite accurate outcome. Finally, both of the approaches have been compared and both of them yield promising results. Numerical modeling yields more detailed results which can be used for further investigations and it can explain different observed behaviors of hydraulic fracturing in naturally fractured reservoirs as well as activation of natural fractures. Also, the potential conditions that may lead to hydraulic fracturing operation failure can be investigated through numerical modeling but it is computationally more expensive and time-consuming than artificial neural network approach. In another hand, since artificial neural network approach is mainly data-driven it can be of great use in real-time experimental studies and field hydraulic fracturing in naturally fractured reservoirs. So, as one may conclude easily, numerical modeling and artificial intelligence both have some positive and negative points; hence simultaneous use of these methods will lead to both technical and economical advantages in hydraulic fracturing operation especially in the presence of natural fractures.

## Author details

Reza Keshavarzi and Reza Jahanbakhshi

Young Researchers and Elites Club, Science and Research Branch, Islamic Azad University, Tehran, Iran

## References

- [1] Liu, E. (2005). Effects of fracture aperture and roughness on hydraulic and mechanical properties of rocks: implication of seismic characterization of fractured reservoirs. *Journal of Geophysics and Engineering*, , 2, 38-47.
- [2] Gale, J. F. W, Reed, R. M, & Holder, J. (2007). Natural fractures in the Barnett Shale and their importance for hydraulic fracture treatments, *AAPG Bulletin*, , 91, 603-622.
- [3] Lamont, N, & Jessen, F. (1963). The Effects of Existing Fractures in Rocks on the Extension of Hydraulic Fractures. *JPT*, February., 203-209.
- [4] Blanton, T. L. (1982). An Experimental Study of Interaction Between Hydraulically Induced and Pre-Existing Fractures. SPE 10847. Presented at SPE/DOE unconventional Gas Recovery Symposium, Pittsburg, Pennsylvania, May., 16-18.
- [5] Warpinski, N. R, & Teufel, L. W. (1987). Influence of Geologic Discontinuities on Hydraulic Fracture Propagation. *JPT* February., 209-220.
- [6] Zhou, J, Chen, M, Jin, Y, & Zhang, G. (2008). Analysis of fracture propagation behavior and fracture geometry using a tri-axial fracturing system in naturally fractured reservoirs. *International Journal of Rock Mechanics & Mining Sciences* (45) 1143-1152.
- [7] Athavale, A. S, & Miskimins, J. L. (2008). Laboratory Hydraulic Fracturing Tests on Small Homogeneous and Laminated Blocks. 42nd US Rock Mechanics Symposium and 2nd U.S.-Canada Rock Mechanics Symposium, San Francisco, June July 2., 29.
- [8] Zhou and Xue(2011). Experimental investigation of fracture interaction between natural fractures and hydraulic fracture in naturally fractured reservoirs. SPE EUROPEC/EAGE Annual Conference and Exhibition, Vienna, Austin, May , 23-26.
- [9] Akulich, A. V, & Zvyagin, A. V. (2008). Interaction between Hydraulic and Natural Fractures. *Fluid Dynamics*. , 43, 428-435.
- [10] Jeffrey, R. G, & Zhang, X. (2009). Hydraulic Fracture Offsetting in Naturally Fractured Reservoirs: Quantifying a Long-Recognized Process. SPE Hydraulic Fracturing Technology Conference, Woodlands, Texas, USA, January., 19-21.
- [11] Rahman, M. M, Aghighi, A, & Rahman, S. S. (2009). Interaction between Induced Hydraulic Fracture and Pre-Existing Natural Fracture in a Poro-elastic Environment: Effect of Pore Pressure Change and the Orientation of Natural Fracture. SPE 122574. Presented at SPE Asia Pacific Oil and Gas Conference and Exhibition, Indonesia, August., 4-6.
- [12] Dahi Taleghani A. and Olson, J.E. (2009). Numerical Modeling of Multi-Stranded Hydraulic Fracture Propagation: Accounting for the Interaction between Induced and Natural Fractures. SPE 124884. Presented at SPE Annual Technical Conference and Exhibition, New Orleans, Louisiana, USA, October., 4-7.

- [13] Chuprakov, D. A, Akulich, A. V, & Siebrits, E. (2010). Hydraulic Fracture Propagation in a Naturally Fractured Reservoir. SPE Oil and Gas India Conference, Mumbai, India, January., 20-22.
- [14] McLennan, J, Tran, D, Zhao, N, Thakur, S, Deo, M, Gil, I, & Damjanac, B. (2010). Modeling Fluid Invasion and Hydraulic Fracture Propagation in Naturally Fractured Rock: A Three-Dimensional Approach. SPE 127888, presented at International Symposium and Exhibition on Formation Damage Control held in Lafayette, Louisiana, USA, February., 10-12.
- [15] Min, K. S, Zhang, Z, & Ghassemi, A. (2010). Numerical Analysis of Multiple Fracture Propagation in Heterogeneous Rock. 44th US Rock Mechanics Symposium and 5th U.S.-Canada Rock Mechanics Symposium, Salt Lake City, UT, June , 27-30.
- [16] Keshavarzi, R, & Mohammadi, S. (2012). A New Approach for Numerical Modeling of Hydraulic Fracture Propagation in Naturally Fractured Reservoirs. SPE/EAGE European Unconventional Resources Conference and Exhibition Vienna, Austria, March., 20-22.
- [17] Keshavarzi, R, Mohammadi, S, & Bayesteh, H. (2012). Hydraulic Fracture Propagation in Unconventional Reservoirs: The Role of Natural Fractures. 46th ARMA Symposium, Chicago, June., 24-27.
- [18] Keshavarzi, R, & Jahanbakhshi, R. (2013). Real-Time Prediction of Complex Hydraulic Fracture Behaviour in Unconventional Naturally Fractured Reservoirs. SPE Middle East Unconventional Gas Conference and Exhibition, Muscat, Oman, January., 28-30.
- [19] Stadulis, J. M. (1995). Development of a Completion Design to Control Screenouts Caused by Multiple Near-Wellbore Fractures. SPE 29549. Presented at Rocky Mountain Regional/Low Permeability Reservoirs Symposium and Exhibition, Denver, March., 19-22.
- [20] Britt, L. K, & Hager, C. J. (1994). Hydraulic Fracturing in a Naturally Fractured Reservoir. SPE 28717. Presented at SPE International Petroleum Conference and Exhibition, Veracruz, Mexico, October., 10-13.
- [21] Rodgerson, J. I. (2000). Impact of Natural Fractures in Hydraulic Fracturing of Tight Gas Sands. SPE 59540 Presented at SPE Permian Basin Oil and Gas Recovery Conference, Midland, Texas, March., 21-23.
- [22] Jeffrey, R. G, Zhang, X, & Bungler, A. P. (2010). Hydraulic fracturing of naturally fractured reservoirs. Thirty-Fifth Workshop on Geothermal Reservoir Engineering Stanford University, Stanford, California, February , 1-3.
- [23] Economides, M. J. (1995). *A practical companion to reservoir stimulation*. Elsevier Science Publishers. USA.

- [24] Potluri, N, Zhu, D, & Hill, A. D. (2005). Effect of natural fractures on hydraulic fracture propagation. Presented at the SPE European formation damage Conference, Scheveningen, Netherlands, May., 25-27.
- [25] Renshaw, C. E, & Pollard, D. D. (1995). An Experimentally Verified Criterion for Propagation across Unbonded Frictional Interfaces in Brittle, Linear Elastic Materials. *International Journal of Rock Mechanics Mining Science and Geomechanics*, (32) 237-249.
- [26] Gale, J. F. W, & Laubach, S. (2010). Natural fracture study: Implications for development of effective drilling and completion technologies. The University of Texas at Austin, USA.
- [27] Mohammadi, S. (2008). Extended finite element method for fracture analysis of structure. Blackwell Publishing, UK.
- [28] Moran, B, & Shih, C. F. (1987). A general treatment of crack tip contour integrals. *International Journal of Fracture*, , 35, 295-310.
- [29] Sukumar, N, & Prévost, J. H. (2003). Modeling quasi-static crack growth with the extended finite element method Part I: Computer implementation. *International Journal of Solids and Structures*, , 40, 7513-7537.
- [30] Belytschko, T, & Black, T. (1999). Elastic crack growth in finite elements with minimal remeshing. *International Journal of Fracture Mechanics*, , 45, 601-620.
- [31] Moës, N, Dolbow, J, & Belytschko, T. (1999). A finite element method for crack growth without remeshing. *International Journal for Numerical Methods in Engineering* , 46(1), 131-150.
- [32] DauxCh., Moës, N., Dolbow, J., Sukumar, N. and Belytschko, T. (2000). *International Journal for Numerical Methods in Engineering*, , 48(12), 1741-1760.
- [33] Sadiq, T, & Nashawi, I. S. (2000). Using Neural Networks for Prediction of Formation Fracture Gradient. SPE 65463. Presented at SPE/Petroleum Society of CIM International Conference on Horizontal Well Technology held in Calgary, Alberta, Canada, November., 6-8.
- [34] Keshavarzi, R, Jahanbakhshi, R, & Rashidi, M. (2011). Predicting Formation Fracture Gradient in Oil and Gas Wells: A Neural Network Approach. 45th ARMA Symposium, San Francisco, June., 26-29.
- [35] Mohaghegh, S. (2000). Virtual-Intelligence Applications in Petroleum Engineering, Parts Artificial Neural Networks. SPE 58046, *Distinguished Author Series*. doi:, 1.
- [36] Demuth, H, & Beale, M. (1998). *Neural network toolbox for use with MATLAB*. User's Guide, Fifth Printing, Version 3. USA: Mathworks, Inc.
- [37] Hagan, M. T, Demuth, H. B, & Beale, M. (1996). *Neural Network Design*. USA, Boston: PWS Publishing Company.

- [38] Doraisamy, H, Ertekin, T, & Grader, A. S. (1998). Key Parameters Controlling the Performance of neuron- Simulation Applications in Field Development. SPE 51079. Presented at SPE eastern Regional Meeting, Pittsburgh, Pennsylvania, November., 9-11.
- [39] Centilmen, A, Ertekin, T, & Grader, A. S. (1999). Applications of Neural-networks in Multi-well Field Development. SPE 56624. Presented at SPE Annual Technical Conference and Exhibition, Houston, Texas, October. doi:
- [40] Ali, J. K. (1994). Neural Networks: A New Tool for the Petroleum Industry?.SPE 27561. Presented at European Petroleum Computer Conference held in Aberdeen, U.K., March., 15-17.
- [41] Fawcett, T. (2006). *An introduction to ROC analysis*. Pattern Recognition Letters , 27, 861-874.
- [42] Taylor, J. R. (1999). *An Introduction to Error Analysis: The Study of Uncertainties in Physical Measurements*. University Science Books. , 128-129.
- [43] Al-fattah, S. M, & Startzman, R. A. (2001). Predicting Natural Gas Production Using Artificial Neural Network. SPE 68593. Presented at SPE Hydrocarbon Economics and Evaluation Symposium, Dallas, Texas, April., 2-3.

IntechOpen